

Effective CFS-PML Formulations Based on 2-D TE_ϕ BOR-FDTD for the Drude Model

Jianxiong Li^{1,2,*} and Wei Jiao^{1,2}

¹ School of Electronics and Information Engineering
Tianjin Polytechnic University, Tianjin, 300387, China
lijianxiong@tjpu.edu.cn

² Tianjin Key Laboratory of Optoelectronic Detection Technology and Systems
Tianjin, 300387, China

Abstract — Effective formulations of the complex frequency-shifted perfectly matched layer (CFS-PML) based on the two-dimensional (2-D) TE_ϕ body of revolution finite-difference time-domain (BOR-FDTD), named as the BOR-CFS-PML, are proposed to truncate the Drude media. The auxiliary differential equation (ADE) method and the trapezoidal recursive convolution (TRC) method are applied to the implementation of the BOR-CFS-PML. The proposed formulations have good performance in attenuating low-frequency evanescent waves and reducing late-time reflections. A numerical test is provided to validate the effectiveness of the proposed algorithm.

Index Terms — Auxiliary differential equation (ADE), body of revolution (BOR), complex frequency-shifted perfectly matched layer (CFS-PML), finite-difference time-domain (FDTD), trapezoidal recursive convolution (TRC).

I. INTRODUCTION

The body of revolution finite-difference time-domain (BOR-FDTD) method [1],[2] plays an important role in simulating electromagnetic wave propagation in rotationally symmetric geometries. The BOR-FDTD has an advantage of simplifying an original three-dimensional (3-D) problem to a two-dimensional (2-D) problem, so that it saves much running time.

When the open region problems are simulated, an effective absorbing boundary condition is necessary. The perfectly matched layer (PML) was firstly introduced by Berenger in [4]. Next, the stretched coordinate PML (SC-PML) with simple implementation in the corners and edges of the PML regions was presented in [5]. However, the SC-PML had a drawback of the inefficiency in attenuating the evanescent waves [6],[7]. To overcome the shortcoming of the SC-PML, the complex frequency-shifted PML (CFS-PML) [8] was proposed to efficiently

damp the low-frequency evanescent waves and late-time reflections [6].

To analyze the Drude model and other dispersive models, the recursive convolution (RC) method [9],[10], the piecewise linear RC (PLRC) method [11] and the trapezoidal RC (TRC) method [12,13] have been explored to realize the frequency-dependent FDTD method. Especially, the TRC method has the advantages of high accuracy and simplicity.

In this paper, effective formulations of the CFS-PML based on the (2-D) TE_ϕ BOR-FDTD, named here as the BOR-CFS-PML, are proposed. The formulations of the BOR-CFS-PML utilize the auxiliary differential equation (ADE) method [14] and the TRC method to truncate the Drude media. The results of the numerical example show that the BOR-CFS-PML has much better absorbing performance than the SC-PML based on the BOR-FDTD.

II. FORMULATIONS

In the cylinder coordinate, the complex spatial coordinate-stretching variables are defined as:

$$\tilde{r} = r_1 + \int_{r_1}^r S_r(r') dr', \quad (1)$$

$$\tilde{z} = z_1 + \int_{z_1}^z S_z(z') dz', \quad (2)$$

where r_1 and z_1 are the interfaces between the FDTD and the PML grids along the directions of r and z , respectively, and S_η ($\eta = r, z$) are the CFS-PML variables given by:

$$S_\eta = \kappa_\eta + \frac{\sigma_\eta}{\alpha_\eta + j\omega\epsilon_0}, \quad (3)$$

where σ_η and α_η are positive real and κ_η is real and ≥ 1 .

In 2-D TE_ϕ case, based on the SC-PML formulations [5], the frequency-domain modified Maxwell's equations

in the Drude media can be written as:

$$j\omega D_r = -\frac{1}{S_z} \cdot \frac{\partial H_\phi}{\partial z}, \quad (4)$$

$$j\omega D_z = \frac{1}{S_r} \cdot \frac{\partial H_\phi}{\partial r} + \frac{H_\phi}{\tilde{r}}, \quad (5)$$

$$-j\omega\mu_0 H_\phi = \frac{1}{S_z} \cdot \frac{\partial E_r}{\partial z} - \frac{1}{S_r} \cdot \frac{\partial E_z}{\partial r}. \quad (6)$$

The frequency-domain electric flux density D_η ($\eta = r, z$) are given by:

$$D_\eta = \varepsilon_0 \varepsilon_r(\omega) E_\eta, \quad (7)$$

where $\varepsilon_r(\omega)$ is the complex relative permittivity of the Drude model defined as:

$$\varepsilon_r(\omega) = 1 + \frac{\omega_p^2}{-\omega^2 + j\omega\Gamma}, \quad (8)$$

where ω_p is the Drude pole frequency and Γ is the damping constant.

By using the partial fraction expansion, S_η^{-1} can be expressed as:

$$S_\eta^{-1} = \frac{1}{\kappa_\eta} - \frac{\frac{\sigma_\eta}{\kappa_\eta^2 \varepsilon_0}}{j\omega + \frac{\alpha_\eta + \sigma_\eta}{\varepsilon_0} + \frac{\sigma_\eta}{\kappa_\eta \varepsilon_0}} = \frac{1}{\kappa_\eta} - \frac{\beta_\eta}{j\omega + \varphi_\eta}, \quad (9)$$

where

$$\beta_\eta = \frac{\sigma_\eta}{\kappa_\eta^2 \varepsilon_0} \quad \text{and} \quad \varphi_\eta = \frac{\alpha_\eta}{\varepsilon_0} + \frac{\sigma_\eta}{\kappa_\eta \varepsilon_0}.$$

By submitting (9) into (4)-(6) and using the inverse Fourier transformation and the ADE method, ones obtains:

$$\frac{\partial D_r}{\partial t} = -\frac{1}{\kappa_z} \cdot \frac{\partial H_\phi}{\partial z} + F_{rz}, \quad (10)$$

$$\frac{\partial D_z}{\partial t} = \frac{1}{\kappa_r} \cdot \frac{\partial H_\phi}{\partial r} - G_{zr} + \frac{1}{\lambda_r} \cdot \frac{H_\phi}{r} - P_{zr}, \quad (11)$$

$$-\mu_0 \frac{\partial H_\phi}{\partial t} = \frac{1}{\kappa_z} \cdot \frac{\partial E_r}{\partial z} - Q_{\phi z} - \frac{1}{\kappa_r} \cdot \frac{\partial E_z}{\partial r} + Q_{\phi r}, \quad (12)$$

where F_{rz} , G_{zr} , P_{zr} , $Q_{\phi z}$ and $Q_{\phi r}$ are the auxiliary variables expressed as follows:

$$\frac{\partial F_{rz}}{\partial t} + \varphi_z F_{rz} = \beta_z \cdot \frac{\partial H_\phi}{\partial z}, \quad (13)$$

$$\frac{\partial G_{zr}}{\partial t} + \varphi_r G_{zr} = \beta_r \cdot \frac{\partial H_\phi}{\partial r}, \quad (14)$$

$$\frac{\partial P_{zr}}{\partial t} + \left(\frac{\alpha_r}{\varepsilon_0} + \frac{\theta_r}{\varepsilon_0 \lambda_r} \right) P_{zr} = \frac{\theta_r}{\varepsilon_0 \lambda_r^2} \cdot \frac{H_\phi}{r}, \quad (15)$$

$$\frac{\partial Q_{\phi z}}{\partial t} + \varphi_z Q_{\phi z} = \beta_z \cdot \frac{\partial E_r}{\partial z}, \quad (16)$$

$$\frac{\partial Q_{\phi r}}{\partial t} + \varphi_r Q_{\phi r} = \beta_r \cdot \frac{\partial E_z}{\partial r}, \quad (17)$$

where

$$\lambda_r = \frac{1}{r} \cdot \left(r_1 + \int_{r_1}^r \kappa_r(r') dr' \right) \quad \text{and} \quad \theta_r = \frac{1}{r} \cdot \int_{r_1}^r \sigma_r(r') dr'.$$

Using the BOR-FDTD scheme and the TRC method [12] to discretize (10)-(17), ones obtains:

$$\begin{aligned} E_r^{n+1}(i+\frac{1}{2}, k) &= a_1 E_r^n(i+\frac{1}{2}, k) + a_2 \psi_r^n(i+\frac{1}{2}, k) \\ &\quad - c_{z1}(k) \left[H_\phi^{n+1/2}(i+\frac{1}{2}, k+\frac{1}{2}) - H_\phi^{n+1/2}(i+\frac{1}{2}, k-\frac{1}{2}) \right] \\ &\quad + c_{z2}(k) F_{rz}^n(i+\frac{1}{2}, k), \end{aligned} \quad (18)$$

$$\begin{aligned} \psi_r^{n+1}(i+\frac{1}{2}, k) &= \frac{\Delta \chi^0}{2} \left[E_r^{n+1}(i+\frac{1}{2}, k) + E_r^n(i+\frac{1}{2}, k) \right] \\ &\quad + e^{-\Gamma \Delta t} \psi_r^n(i+\frac{1}{2}, k), \end{aligned} \quad (19)$$

$$\begin{aligned} E_z^{n+1}(i, k+\frac{1}{2}) &= a_1 E_z^n(i, k+\frac{1}{2}) + a_2 \psi_z^n(i, k+\frac{1}{2}) \\ &\quad + c_{r1}(i) \left[H_\phi^{n+1/2}(i+\frac{1}{2}, k+\frac{1}{2}) - H_\phi^{n+1/2}(i-\frac{1}{2}, k+\frac{1}{2}) \right] \\ &\quad + w_{r1}(i) \cdot \frac{H_\phi^{n+1/2}(i+\frac{1}{2}, k+\frac{1}{2}) + H_\phi^{n+1/2}(i-\frac{1}{2}, k+\frac{1}{2})}{2i} \\ &\quad - c_{r2}(i) G_{zr}^n(i, k+\frac{1}{2}) - w_{r2}(i) P_{zr}^n(i, k+\frac{1}{2}), \end{aligned} \quad (20)$$

$$\begin{aligned} \psi_z^{n+1}(i, k+\frac{1}{2}) &= \frac{\Delta \chi^0}{2} \left[E_z^{n+1}(i, k+\frac{1}{2}) + E_z^n(i, k+\frac{1}{2}) \right] \\ &\quad + e^{-\Gamma \Delta t} \psi_z^n(i, k+\frac{1}{2}), \end{aligned} \quad (21)$$

$$\begin{aligned} H_\phi^{n+1/2}(i+\frac{1}{2}, k+\frac{1}{2}) &= H_\phi^{n-1/2}(i+\frac{1}{2}, k+\frac{1}{2}) \\ &\quad - d_{z1}(k+\frac{1}{2}) \left[E_r^n(i+\frac{1}{2}, k+1) - E_r^n(i+\frac{1}{2}, k) \right] \\ &\quad + d_{r1}(i+\frac{1}{2}) \left[E_z^n(i+1, k+\frac{1}{2}) - E_z^n(i, k+\frac{1}{2}) \right] \\ &\quad + d_{z2}(k+\frac{1}{2}) Q_{\phi z}^{n-1/2}(i+\frac{1}{2}, k+\frac{1}{2}) \\ &\quad - d_{r2}(i+\frac{1}{2}) Q_{\phi r}^{n-1/2}(i+\frac{1}{2}, k+\frac{1}{2}), \end{aligned} \quad (22)$$

$$\begin{aligned} F_{rz}^{n+1}(i+\frac{1}{2}, k) &= a_z(k) F_{rz}^n(i+\frac{1}{2}, k) \\ &\quad + b_z(k) \left[H_\phi^{n+1/2}(i+\frac{1}{2}, k+\frac{1}{2}) - H_\phi^{n+1/2}(i+\frac{1}{2}, k-\frac{1}{2}) \right], \end{aligned} \quad (23)$$

$$\begin{aligned} G_{zr}^{n+1}(i, k+\frac{1}{2}) &= a_r(i) G_{zr}^n(i, k+\frac{1}{2}) \\ &\quad + b_r(i) \left[H_\phi^{n+1/2}(i+\frac{1}{2}, k+\frac{1}{2}) - H_\phi^{n+1/2}(i-\frac{1}{2}, k+\frac{1}{2}) \right], \end{aligned} \quad (24)$$

$$\begin{aligned} P_{zr}^{n+1}(i, k+\frac{1}{2}) &= u_r(i) P_{zr}^n(i, k+\frac{1}{2}) \\ &\quad + v_r(i) \cdot \frac{H_\phi^{n+1/2}(i+\frac{1}{2}, k+\frac{1}{2}) + H_\phi^{n+1/2}(i-\frac{1}{2}, k+\frac{1}{2})}{2i}, \end{aligned} \quad (25)$$

$$\begin{aligned} Q_{\phi z}^{n+1/2}(i+\frac{1}{2}, k+\frac{1}{2}) &= a_z(k+\frac{1}{2}) Q_{\phi z}^{n-1/2}(i+\frac{1}{2}, k+\frac{1}{2}) \\ &\quad + b_z(k+\frac{1}{2}) \left[E_r^n(i+\frac{1}{2}, k+1) - E_r^n(i+\frac{1}{2}, k) \right], \end{aligned} \quad (26)$$

$$\begin{aligned} Q_{\phi r}^{n+1/2}(i+\frac{1}{2}, k+\frac{1}{2}) &= a_r(i+\frac{1}{2}) Q_{\phi r}^{n-1/2}(i+\frac{1}{2}, k+\frac{1}{2}) \\ &\quad + b_r(i+\frac{1}{2}) \left[E_z^n(i+1, k+\frac{1}{2}) - E_z^n(i, k+\frac{1}{2}) \right]. \end{aligned} \quad (27)$$

It can be seen that (11) includes a singularity when $r=0$ for the $1/r$ term. The proposed update equation to

solve the problem [2] is:

$$E_z^{n+1}(0, k + \frac{1}{2}) = a_1 E_z^n(0, k + \frac{1}{2}) + a_2 \psi_z^n(0, k + \frac{1}{2}) + \frac{a_2 \Delta t}{\epsilon_0} \cdot \frac{4}{\Delta r} \cdot H_\phi^{n+1/2}(\frac{1}{2}, k + \frac{1}{2}). \quad (28)$$

The corresponding coefficients in (18)-(28) are listed as follows:

$$a_1 = a_2 \left(1 - \frac{\chi^0}{2}\right), \quad a_2 = \left(1 + \frac{\chi^0}{2}\right)^{-1},$$

$$\chi^0 = \frac{\omega_p^2}{\Gamma} \Delta t - \frac{\omega_p^2}{\Gamma^2} (1 - e^{-\Gamma \Delta t}), \quad \Delta \chi^0 = -\frac{\omega_p^2}{\Gamma^2} (1 - e^{-\Gamma \Delta t})^2,$$

$$a_\eta = \frac{2 - \varphi_\eta \Delta t}{2 + \varphi_\eta \Delta t}, \quad b_\eta = \frac{2\beta_\eta \Delta t}{2 + \varphi_\eta \Delta t} \cdot \frac{1}{\Delta \eta},$$

$$u_r = \frac{2\epsilon_0 \lambda_r - \alpha_r \Delta t \lambda_r - \theta_r \Delta t}{2\epsilon_0 \lambda_r + \alpha_r \Delta t \lambda_r + \theta_r \Delta t},$$

$$v_r = \frac{2\theta_r \Delta t}{\lambda_r [2\epsilon_0 \lambda_r + \alpha_r \Delta t \lambda_r + \theta_r \Delta t]} \cdot \frac{1}{\Delta r},$$

$$c_{\eta 1} = \frac{a_2 \Delta t}{\epsilon_0} \left(\frac{1}{\kappa_\eta \Delta \eta} - \frac{b_\eta}{2} \right), \quad c_{\eta 2} = \frac{a_2 \Delta t}{2\epsilon_0} (1 + a_\eta),$$

$$d_{\eta 1} = \frac{\Delta t}{\mu_0} \left(\frac{1}{\kappa_\eta \Delta \eta} - \frac{b_\eta}{2} \right), \quad d_{\eta 2} = \frac{\Delta t}{2\mu_0} (1 + a_\eta),$$

$$w_{r1} = \frac{a_2 \Delta t}{\epsilon_0} \left(\frac{1}{\lambda_r \Delta r} - \frac{b_{\theta r}}{2} \right), \quad w_{r2} = \frac{a_2 \Delta t}{2\epsilon_0} (1 + a_{\theta r}),$$

where $\Delta \eta$ ($\eta = r, z$) are the space cell size and Δt is the time step.

III. NUMERICAL RESULTS

A numerical example is provided to validate the effectiveness of the proposed BOR-CFS-PML formulations. The model structure of the numerical example is presented in Fig. 1. The BOR-CFS-PML with 10-cell-thick layers is used to truncate the FDTD computation domain filled with the Drude media with $\omega_p = 2\pi \times 28.7$ Grad/s and $\Gamma = 20$ Grad/s, which occupies 60×80 cells. The space cell size is $\Delta r = \Delta z = 2 \times 10^{-4}$ m and the time step is $\Delta t = 4.48 \times 10^{-13}$ s. In this simulation, the excite source, which is located at (10, 50) as shown in Fig. 1, is a modulated Gaussian pulse whose center frequency is 35 GHz and maximum interesting frequency is 70 GHz. In the PML domain, σ_η and κ_η are scaled using an m -order polynomial scaling and α_η is a constant. To obtain the low reflection, the BOR-CFS-PML parameters $\kappa_{\eta, \max} = 10$, $\alpha_\eta = 0.6$, $\sigma_{\eta, \max} = \sigma_{\eta, \text{ratio}} (m+1)/(150\pi \Delta \eta)$, $\sigma_{\eta, \text{ratio}} = 1.4$, $m = 2$ are selected empirically. The simulation is operated for 2240 ps.

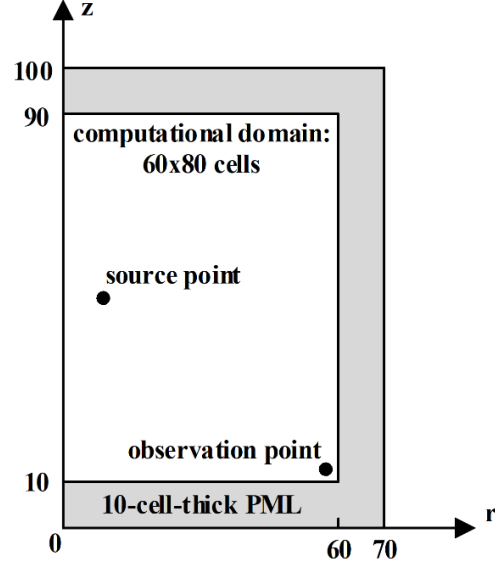


Fig. 1. The model structure of the numerical example.

The relative reflection error of the BOR-CFS-PML in the time-domain is shown in Fig. 2. The relative reflection error is calculated at an observation point located at (59, 11) as:

$$R_{\text{dB}}(t) = 20 \log_{10} \left| \frac{H_\phi^R(t) - H_\phi^T(t)}{\max(H_\phi^R(t))} \right|, \quad (29)$$

where $H_\phi^T(t)$ represents the value calculated in the test domain, $H_\phi^R(t)$ is the reference solution based on the extended 260x480-cell FDTD computational domain terminated by additional 128-cell-thick PML layers. For comparing, the SC-PML based on the BOR-FDTD, named here as the BOR-SC-PML, is also computed by using the same PML parameters except $\alpha_\eta = 0$. Compared with the BOR-SC-PML, the BOR-CFS-PML has better performance in reducing late-time reflection error. Specially, it has about 60 dB improvement near $t = 1500$ ps.

Figure 3 shows the reflection coefficients in the frequency-domain with the BOR-CFS-PML and the BOR-SC-PML. The reflection coefficients are calculated at the same observation point by using:

$$R_{\text{dB}}(f) = 20 \log_{10} \left| \frac{F[H_\phi^R(t) - H_\phi^T(t)]}{F[H_\phi^R(t)]} \right|, \quad (30)$$

where the operator $F[*]$ is the symbol of the Fourier transformation. The maximum reflection coefficient of the BOR-CFS-PML is -68 dB in the interesting frequency range. Within the low-frequency, the BOR-CFS-PML holds significant improvement compared with the BOR-SC-PML.

In conclusion, the BOR-CFS-PML holds the remarkable advantages in attenuating low-frequency evanescent waves and reducing late-time reflections over the BOR-SC-PML.

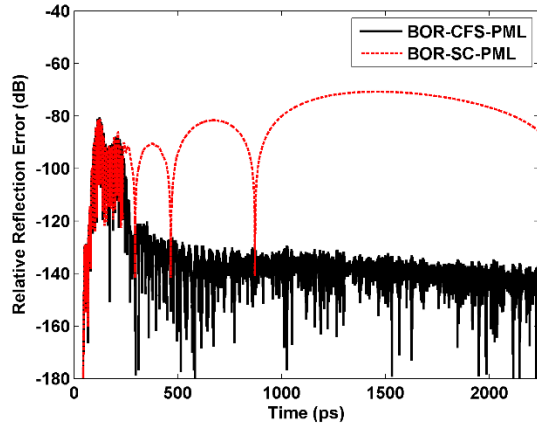


Fig. 2. Relative reflection errors versus time of the BOR-CFS-PML and the BOR-SC-PML for truncating the Drude media. (Two curves almost overlap before 237ps).

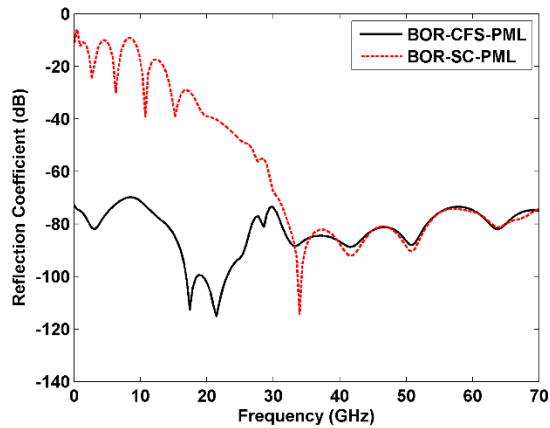


Fig. 3. Reflection coefficients versus frequency of the BOR-CFS-PML and the BOR-SC-PML for truncating the Drude media. (Two curves almost overlap after 35 GHz).

IV. CONCLUSION

An effective implementation of the BOR-CFS-PML, which takes advantage of the ADE method and the TRC method to terminate the Drude media, is presented. It is confirmed in the numerical example that the proposed BOR-CFS-PML is efficient in the absorption of the low-frequency evanescent waves and the reduction of late-time reflections.

ACKNOWLEDGMENT

This work was supported by the National Natural Science Foundation of China (Grant No. 61372011) and

the Program for Innovative Research Team in University of Tianjin (Grant No. TD13-5040).

REFERENCES

- [1] A. Taflove and S. C. Hagness, *Computational Electrodynamics: The Finite-Difference Time-Domain Method*. 3rd ed., Norwood, MA: Artech House, 2005.
- [2] M. F. Hadi, A. Z. Elsherbeni, M. J. Piket-May, and S. F. Mahmoud, "Radial waves based dispersion analysis of the body-of-revolution FDTD method," *IEEE Trans. Antennas & Propagation*, vol. 65, no. 2, pp. 721-729, Feb. 2017.
- [3] Y. Chen, R. Mittra, and P. Harms, "Finite-difference time-domain algorithm for solving Maxwell's equations in rotationally symmetric geometries," *IEEE Trans. Microw. Theory Tech.*, vol. 44, no. 6, pp. 832-839, June 1996.
- [4] J. P. Berenger, "A perfectly matched layer for the absorption of electromagnetic waves," *J. Comp. Phys.*, vol. 114, no. 2, pp. 185-200, Oct. 1994.
- [5] W. C. Chew and W. H. Weedon, "A 3D perfectly matched medium from modified Maxwell's equations with stretched coordinates," *Microw. Opt. Technol. Lett.*, vol. 7, no. 13, pp. 599-604, Sep. 1994.
- [6] J. P. Berenger, "Numerical reflection from FDTD-PMLs: A comparison of the split PML with the unsplit and CFS PMLs," *IEEE Trans. Antennas Propag.*, vol. 50, no. 3, pp. 258-265, Mar. 2002.
- [7] J. P. Berenger, "Evanescent waves in PML's: Origin of the numerical reflection in wave-structure interaction problems," *IEEE Trans. Antennas Propag.*, vol. 47, no. 10, pp. 1497-1503, Oct. 1999.
- [8] M. Kuzuoglu and R. Mittra, "Frequency dependence of the constitutive parameters of causal perfectly matched anisotropic absorbers," *IEEE Microw. Guided Wave Lett.*, vol. 6, no. 12, pp. 447-449, Dec. 1996.
- [9] R. Luebbers, F. P. Hunsberger, K. S. Kunz, R. B. Standler, and M. Schneider, "A frequency-dependent finite-difference time-domain formulation for dispersive materials," *IEEE Trans. Electromag. Compat.*, vol. 32, no. 3, pp. 222-227, Aug. 1990.
- [10] R. J. Luebbers, F. Hunsberger, and K. S. Kunz, "A frequency-dependent finite-difference time-domain formulation for transient propagation in plasma," *IEEE Trans. Antennas Propag.*, vol. 39, no. 1, pp. 29-34, Jan. 1991.
- [11] D. F. Kelley and R. J. Luebbers, "Piecewise linear recursive convolution for dispersive media using FDTD," *IEEE Trans. Antennas Propag.*, vol. 44, no. 6, pp. 792-797, June 1996.
- [12] R. Siushansian and J. LoVetri, "A comparison of numerical techniques for modeling electromag-

netic dispersive media,” *IEEE Microw. Guided Wave Lett.*, vol. 5, no. 12, pp. 426-428, Dec. 1995.

- [13] R. Siushansian and J. LoVetri, “Efficient evaluation of convolution integrals arising in FDTD formulations of electromagnetic dispersive media,” *J. Electromag. Waves Applicat.*, vol. 11, pp. 101-117, 1997.
- [14] O. Ramadan, “Auxiliary differential equation formulation: An efficient implementation of the perfectly matched layer,” *IEEE Microw. Wireless Compon. Lett.*, vol. 13, no. 2, pp. 69-71, Feb. 2003.



Jianxiong Li received the B.Sc. and M.Sc. degrees in Physics in 1991 and 1994, respectively, and obtained the Ph.D. degree in Communication and Information System in 2007, from Tianjin University, Tianjin, China. His main research interests are in computational electromag-

netics, wireless communication and antenna.



Wei Jiao received the B.Sc. degree in Communication Engineering in 2015 from Tianjin Polytechnic University, Tianjin, China. He is currently pursuing the M.Sc. degree in the same university. His main research interests are in computational electromagnetics.